

Impact of a modified implant macrogeometry on biomechanical parameters and bone-related markers in rats

Mounir Colares MUSSI^(a) 
Fernanda Vieira RIBEIRO^(a) 
Monica Grazieli CORRÊA^(a) 
Cristiane Ribeiro SALMON^(a) 
Suzana Peres PIMENTEL^(a) 
Fabiano Ribeiro CIRANO^(a) 
Marcio Zaffalon CASATI^(a) 

^(a)Universidade Paulista, School of Dentistry, Dental Research Division, São Paulo, SP, Brazil.

Abstract: This study investigated the impact of a modified implant macrogeometry on peri-implant healing and its effect on bone-related molecules in rats. Eighteen rats received one implant in each tibia: the control group received implants with conventional macrogeometry and the test group received implants with modified macrogeometry. After 30 days, the implants were removed for biomechanical analysis and the bone tissue around them was collected for quantifying gene expression of OPN, Runx2, β -catenin, BMP-2, Dkk1, and RANKL/OPG. Calcein and tetracycline fluorescent markers were used for analyzing newly formed bone at undecalcified sections of the tibial implants. These fluorescent markers showed continuous bone formation at cortical bone width and sparse new bone formed along the medullary implant surface in both groups. However, higher counter-torque values and upregulation of OPN expression were achieved by test implants when compared to controls. The modified macrogeometry of implants optimized peri-implant healing, favoring the modulation of OPN expression in the osseous tissue around the implants.

Keywords: Dental Implants; Gene Expression; Bone and Bones.

Declaration of Interests: Marcio Zaffalon Casati is currently a scientific advisor for Implacil de Bortoli. All other authors are independent researchers.

Corresponding Author:
Marcio Zaffalon Casati
E-mail: mzcasati@gmail.com

<https://doi.org/10.1590/1807-3107bor-2023.vol37.0044>

Introduction

Dental implant therapy is a rehabilitation strategy largely recognized for restoring missing dentition.¹ Although earlier studies stated that intimate contact between the implant and the bone bed would be important for adequate osseointegration and that primary implant stability could be considered a prerequisite for successful peri-implant bone healing,^{2,3} this scenario has been related to loss of mechanical interlocking between dental implant and bone tissue promoted by widespread bone interfacial remodeling following implant placement.⁴

Innovative bone drilling protocols and different implant macrogeometries, allowing for spaces between the surgical bed and the implant, have since been described as strategies that may favor the clinical outcomes of dental implants.^{5,6} This may be explained by the creation of spaces—“healing chambers”—guaranteed by modified implant macrogeometry; these are occupied by the blood clot instantly following implant placement.

Submitted: September 9, 2021
Accepted for publication: October 17, 2022
Last revision: December 16, 2022



Biologically, while this condition does not favor primary stability, it has been mentioned as a relevant approach for secondary stability.

Although the use of implants as a therapy for dental rehabilitation is well-established as secure and predictable in the long term,^{1,7} some systemic and local circumstances (such as sites with lower bone density) may jeopardize the peri-implant repair process and thus interfere negatively on the predictability and success of dental implants.⁸⁻¹¹ Consequently, innovative strategies based on modified implant macrogeometries could be relevant to optimize dental implant therapy in these conditions. In addition, the literature is scarce regarding the molecular impact of modified implant macrodesign on the pathways involved in bone healing around implants, and no data are available on the influence of the macrogeometry of implant threads on bone-related gene expression, as performed in this investigation. Therefore, it would be important to investigate the behavior of bone markers such as runt-related transcription factor 2 (Runx2), bone morphogenetic protein 2 (BMP-2), osteopontin (OPN), β -catenin, Dickkopf 1 (Dkk1), receptor activator of nuclear factor kappa-B ligand (RANKL), and osteoprotegerin (OPG). Runx2 is thought to be the main transcription factor of osteoblasts,¹² while β -catenin and OPN have osteogenic properties.¹³ Dkk1 is a powerful Wnt antagonist that blocks Wnt/ β -catenin signaling and acts as a negative regulator of osteoblast function.^{14,15} OPG is an important molecule that binds to RANKL preventing RANK/RANKL linkage, which in turn prevents osteoclast differentiation.^{16,17} Both RANKL and OPG participate in the maintenance of bone homeostasis and in the control of bone healing.¹⁶

Considering the evidence highlighting the effect of implant hardware features in bone healing pathways and the encouraging influence of these aspects to maximize osseointegration,^{17,19} this experimental study aimed to evaluate the impact of an implant with modified macrogeometry (with the presence of a healing chamber) on its biomechanical behavior and the biological performance of peri-implant bone tissue. A better comprehension of these aspects

may provide additional support to the clinical use of this approach in the optimization of dental implant therapy.

Methodology

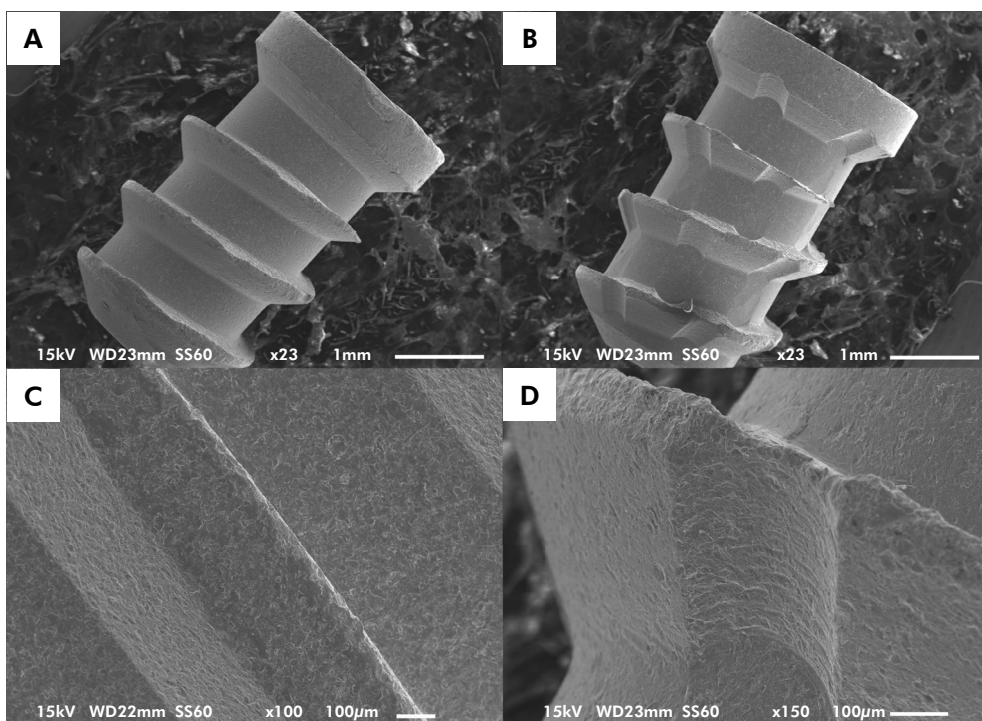
Animals

This study was approved by the University's Animal Care and Use Committee (Process No. 6272060319) and followed the ARRIVE guidelines. This study comprised 18 10-week-old male Wistar rats weighing 338 ± 72 g. The animals were adapted for 15 days and then maintained in temperature-controlled cages with 24-h light-dark cycles for the same period. The animals had water and food ad libitum (Labina, Purina, Paulínia, Brazil) at the University's Animal Facility.

Experimental groups and implant surgery

Two implants were placed in each rat: one in the right and one in the left tibia, in the proximal region of the metaphyses. Each tibia was allocated randomly (using sealed and opaque envelopes) into one of the following groups: control group—implant with conventional macrogeometry; and test group—implant with modified macrogeometry and healing chambers. The implant with modified macrogeometry presented channels that were transversal to the implant threads, while the implant with conventional macrogeometry did not present these channels (Implacil de Bortoli, São Paulo, SP, Brazil); both implants were blasted with titanium oxide microparticles ($\text{Ø}100\text{--}150$ μm) and conditioned with maleic acid. Their surfaces presented a roughness pattern with Ra of 0.56 ± 0.10 μm .²⁰

Briefly, under anesthesia using intramuscular administration of ketamine hydrochloride (0.21 mL/250 g) and xylazine hydrochloride (0.11 mL/250 g), an incision was prepared, and the tibia was exposed by blunt dissection. Implant beds were drilled bicortically using a rotary speed not higher than 1500 rpm. A screw, pelshaped pure aluminum oxide sandblasted titanium implant (4.0 mm long and with a diameter of 2.2 mm), with channels transversal to the implant threads (Implacil de Bortoli, São Paulo, Brazil) (Figure 1), was positioned



A and C) Scanning electron microscopy (JEOL, JSM-6510mca, Tokyo, Japan) of the implants (80-100x) in control group. B and D) Scanning electron microscopy (JEOL, JSM-6510mca, Tokyo, Japan) of the implants (80-100x) in test groups. BC and D) Scanning electron microscopy (JEOL, JSM-6510mca, Tokyo, Japan) of the implants (80-100x) in control and test groups, respectively.

Figure 1. Stereo microscopy of the implants.

in each tibiae until the screw threads were entirely inserted in the bone cortex.²⁰ Sutures were then performed in the soft tissues. Acetaminophen was given for pain control.

Postoperative phase

Animals were monitored every day throughout the experiment. Thirty days following the beginning of the experiment, rats were euthanized by CO₂ inhalation. The tibiae were then dissected to access the implants, which were removed for biomechanical analysis. The bone tissue around the implants was deposited in RNAlater (Ambion Inc., Austin, USA) for gene expression analyses.

Biomechanical analysis of implant removal

Following access to the implant, we attached a torque meter (Mark-10, BGI, USA) with a scale range of 0.1-10 N/cm and divisions of 0.05 N/cm. A wrench was adapted to the implant head to employ torque in the reverse direction of implant placement until total rupture between bone and implant. Torque

values obtained in N/cm were established as the torque required for osseointegration collapse.²¹

Gene expression assay

Bone tissue samples were stored in RNAlater at -70 °C for the assessment of mRNA concentrations of BMP-2, OPN, Runx2, β -catenin, Dkk1 and RANKL/OPG. Total RNA was isolated by the Trizol technique (Gibco BRL, Life Technologies, Rockville, USA) as reported by Conte et al.²² At first, RNA samples were resuspended in diethylpyrocarbonate-treated water and kept at -70 °C. RNA concentration was defined using a spectrophotometer (Nanodrop 1000, Nanodrop Technologies LLC, Wilmington, USA).

Total RNA was DNase-treated (Turbo DNase, Ambion Inc., Austin, USA), and 1 μ g was employed in complementary DNA synthesis. The reaction was performed using the First-Strand cDNA Synthesis kit (Roche Diagnostic Co., Indianapolis, IN, USA). Primers were designed using a probe design software (LightCycler Roche Probe Design, Diagnostics GmbH, Mannheim,

Germany), with sequences (5'–3') and lengths of products (bp) specific to each gene (Table 1). Quantitative polymerase chain reaction (qPCR) was performed with a real-time PCR thermocycler (LightCycler, Roche Diagnostics GmbH, Mannheim, Germany) using FastStart DNA MasterPLUS SYBR Green reagent (Roche Diagnostic Co., Indianapolis, USA); amplification profiles (temperature, time) were defined according to each gene (Table). The outcomes were demonstrated as relative amounts by means of the relative quantification tool, and GAPDH was used as the internal reference gene according to the manufacturer's instructions.

Fluorescence evaluation of bone formation

Three male rats of each experimental group were given an intraperitoneal injection of 20 mg/kg calcein (Sigma-Aldrich, St. Louis, USA) at 24 hours and 21 days after the surgical procedure. Fourteen days after surgery, the rats received 20 mg/kg of tetracycline hydrochloride (Sigma-Aldrich, USA) via intraperitoneal injection. Both fluorescent markers were diluted in 1.4% sodium carbonate solution. The animals were euthanized at day 30 of the experiment. The tibiae were dissected and immediately immersed in 10% buffered formalin solution (pH 7.4) for fixation for 15 days. Samples were washed several times, were gradually dehydrated in a series of ethanol solutions of increasing concentrations, and were then inserted in EMbed 812 resin (EMS, USA). The

middle longitudinal segment of the implants was cut using a low-speed saw (IsoMet 1000, Buehler, USA) to include both medial and lateral cortical bone of the tibiae. The sections were ground to 100 µm and examined by fluorescence microscopy (Eclipse E200, Nikon, Japan). Images of the sections were obtained through a camera (DS-Vi1, Nikon, Japan) coupled to the fluorescence microscope at 4x and 10x magnification.

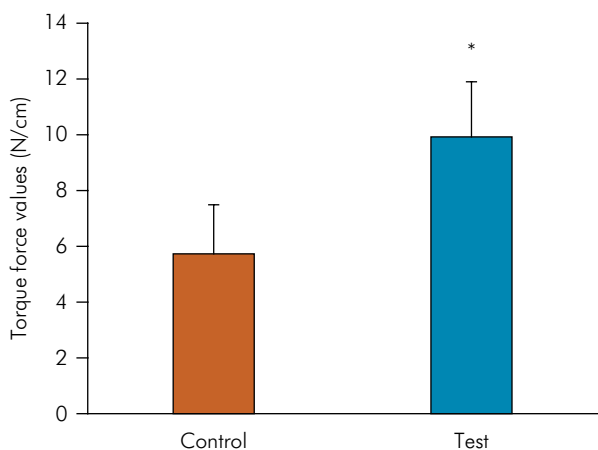
Statistical evaluation

The methodology was reviewed by an independent statistician and all data assessment was executed using SAS software (Program Release 9.3; Cary, USA). Data were evaluated for normality by the Kolmogorov-Smirnov test. Since torque outcomes were normally distributed, parametric methods were used for comparisons. Paired student's t-tests were used for evaluating the biomechanical retention of titanium implants (n = 18 in each group). Considering that the gene expression data (n = 18 in each group) did not achieve normality, non-parametric methods were used for their comparison. Differences in mRNA levels were thus compared using a Wilcoxon test. The number of animals included in the study was based on previous studies that had found significant differences in torque and gene expression levels. The significance level established for all analyses was 5%.

Table. Primer sequences, amplification profiles, and the estimated length of the qPCR product for each gene.

Gene	Sequence (5'–3')	Length of qPCR product	Amplification profile
		bp	temperature, time
Runx2	GCCACTTACCACAGAGC	157	95°C, 10 s/56°C, 8 s/72°C, 7 s
BMP-2	GTCCCTACTGATGATGAGTTTCTC	170	95°C, 10 s/56°C, 8 s/72°C, 8 s
OPN	CCGGATGCAATCGATAGTG	164	95°C, 10 s/56°C, 7 s/72°C, 8 s
β-catenin	ACTCTGAGAACTTGCCG	172	95°C, 10 s/56°C, 8 s/72°C, 8 s
Dkk1	CGGGAATTACTGCAAAAACG	83	95°C, 9 s/59°C, 9 s/72°C, 9 s
RANKL	AGCGCTTCTCAGGAGTT	156	95°C, 5 s/55°C, 4 s/72°C, 6 s
OPG	GCAGAGAAGCACCTAGC	168	95°C, 10 s/56°C, 8 s/72°C, 7 s
GAPDH	TGAGTATGTCGTGGAGTCTACTG	159	95°C, 10 s/56°C, 8 s/72°C, 7 s

qPCR: quantitative polymerase chain reaction; bp: base pairs; Runx2: runt-related transcription factor 2; BMP-2: bone morphogenetic protein 2; OPN: osteopontin; Dkk1: Dickkopf 1; RANKL: receptor activator of the nuclear factor kappa B ligand; OPG: osteoprotegerin; GAPDH: glyceraldehyde-3-phosphate dehydrogenase.



The modified macrogeometry favorably interfered with the biomechanical performance of titanium implants. *statistical differences between groups (paired Student's t-test; $p < 0.05$). Control group ($n = 18$): implant with conventional macrogeometry; test group ($n = 18$): implant with modified macrogeometry and healing chambers.

Figure 2. Biomechanical analysis of implant removal.

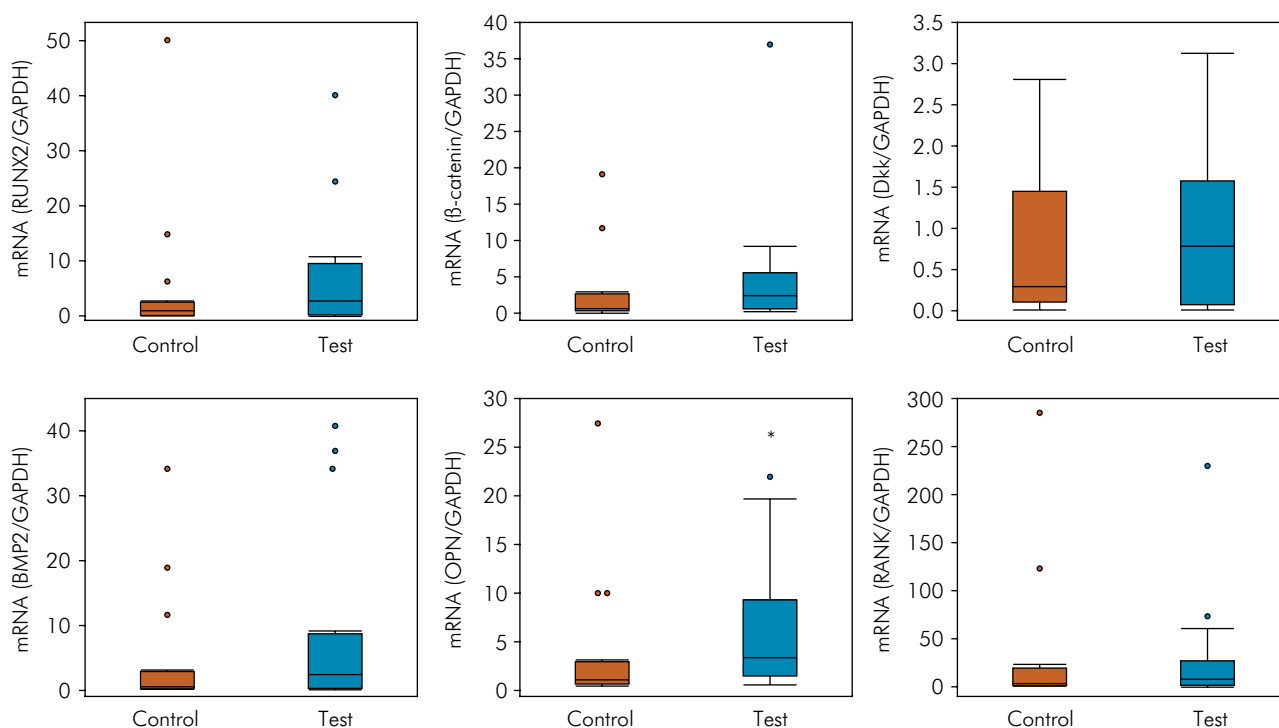
Results

Biomechanical analysis of implant removal

Data analysis showed statistical differences between experimental groups regarding biomechanical analyses, demonstrating that the modified macrogeometry favorably interfered with the biomechanical performance of titanium implants ($p < 0.05$). Figure 2 illustrates the reverse torque data in each group.

Gene expression assay

The gene expression analysis showed that OPN mRNA levels were positively modulated within the bone molecule profile around implants with modified macrogeometry when compared to implants with a conventional thread design ($p < 0.05$). The levels of other bone-related markers did not present significant differences between groups ($p > 0.05$). Figure 3



Gene expression results. OPN levels were positively modulated within the profile of bone molecules in the test group when compared to the control group ($p < 0.05$). The levels of other bone-related markers did not present significant differences between groups ($p > 0.05$). *statistical differences between groups (Wilcoxon test; $p < 0.05$). Control group ($n = 18$): implant with conventional macrogeometry; test group ($n = 18$): implant with modified macrogeometry and healing chambers.

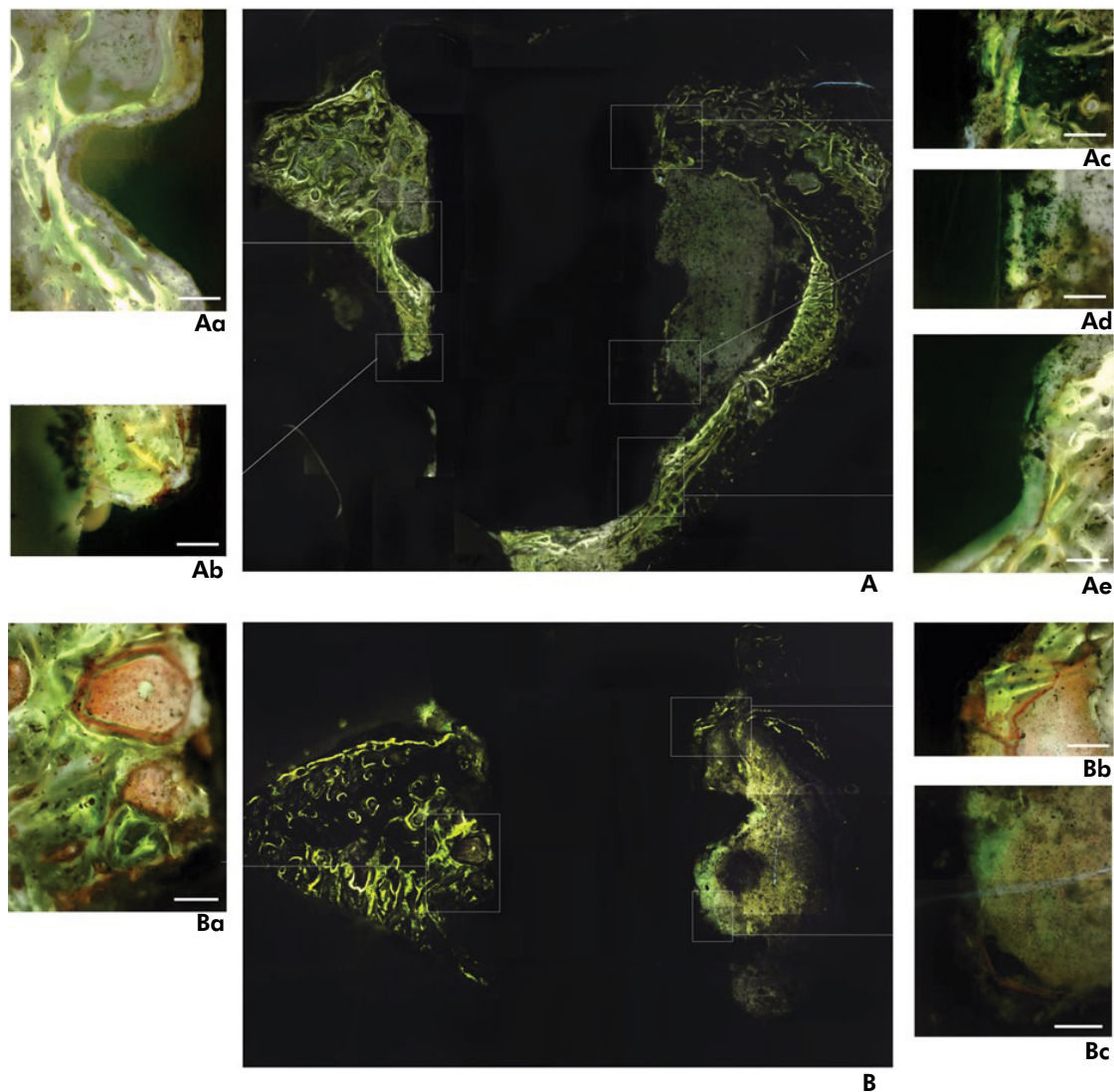
Figure 3. Gene expression assay.

illustrates the mRNA quantification (mean (\pm SD)) of all genes analyzed in each group.

Fluorescence assessment of bone formation

Fluorescent markers were used for a descriptive analysis of bone formation around implants. Green and yellow (calcein and tetracycline markers, respectively) lines observed in tibial bone demonstrated the areas of newly formed bone at

the time of each marker injection. Continuous bone formation was evident in the cortical width, and bright fluorescent labeling was found adjacent to the implant surface in both groups (Figures 4- Aa, Ab, and Ba). New bone was found growing inside the medullary cavity (arrows in Figure 4A) in both groups, while a thin and sparse layer of new bone was found along the medullary implant surface (Figures 4- Ac, Ad, Ae, Bb, and Bc).



Representative images of undecalcified longitudinal sections of the implants. Figures 4A and 4B are photo montages of several images of one section of group A and group B, respectively. Bone formation markers (green lines of calcein staining and yellow lines of tetracycline staining) were observed around both the cortical and medullary surface of implants. Left figures 4- Aa, Ab, and Ba are amplified images of the cortical bone region delimited by squares, while right figures 4- Ac, Ad, Ae, Bb, and Bc are amplified images of the implant surface related to medullary bone. (4A, 4B), 4X magnification; (4Aa-Ae; 4Ba-Bc), 10X magnification; bars = 100 μ m.

Figure 4. Fluorescence assessment of bone formation.

Discussion

Contrarily to the combination of implant dimension and drilling size, which aims for increased juxtaposition between the dental implant and bone tissue instantly following implant placement, the macrogeometry of an implant body with a healing chamber is characterized by plateaus instead of threads, allowing for spaces between the healing chamber/implant surface and the remaining socket walls, optimizing repair around implants.^{21,23} This study evaluated the influence of an implant with modified macrogeometry on its biomechanical behavior and the molecular performance of peri-implant bone tissue. Briefly, implant macrogeometry, modified by the presence of a healing chamber, improved peri-implant bone repair, upregulating OPN expression in the bone tissue around implants when compared to the traditional thread design.

New implant macrogeometries including the concept of a healing chamber have been studied by several researchers.^{6,24,25} In line with the outcomes of the present investigation, previous data have supported that different macrogeometric designs may positively influence bone repair at the interface between bone and implant, enhancing bone formation.¹⁷⁻¹⁹ Earlier experimental research also confirmed that the presence of healing chambers, maintaining spaces filled with blood by using simplified drilling protocols, may improve osseointegration.^{4,6,18,24,26,27} Recently, in an animal study evaluating the biomechanical and histometric impact of implant healing chamber configurations, even though bone-to-implant contact was not improved by the modified macrogeometry, increased bone density was revealed in implants with healing chambers when compared to those with a squared and traditional thread design.²⁶

The assessment of resistance to removal torque is commonly used to determine the interaction force between bone and implant. The data observed in this study concerning the biomechanical analysis of implants showed higher torque values in implants with modified macrogeometry in comparison to conventional implants ($p < 0.05$). Although other experimental studies have reported that healing

chambers introduced in the cortical bone did not improve bone-to-implant contact, increased biomechanical fixation was observed in implants with healing chambers when compared to the conventional thread design,²⁸ which is in accordance with our findings of elevated resistance to removal torque in implants with modified macrogeometry. Meirelles et al.,²⁹ when evaluating bone healing around titanium implants with a chamber design, also demonstrated that the presence of a healing chamber improved wound healing and promoted early repair inside the threads of test implants.

Interestingly, our gene expression analysis showed that the bone tissue around implants with modified macrogeometry presented higher levels of OPN mRNA when compared to that around implants with a conventional thread design ($p < 0.05$). OPN has been reported as an essential molecule involved in bone repair processes, presenting a multiplicity of biological roles during bone healing: it contributes to mesenchymal stem cell recruitment and differentiation, angiogenesis, and mineralization.²⁹⁻³⁵ The accumulation of non-collagenous molecules such as OPN at the bone-implant interface has been previously demonstrated.^{36,37} Evidence supports that OPN stimulates primary mesenchymal stem cell migration around implants in a dose-dependent manner; these cells are able to differentiate toward an osteogenic lineage.^{33,38-41} Recently, it was confirmed that the healing chamber in implants with modified macrogeometry promoted higher osteocyte density, achieving elevated amounts of new bone tissue inside the threads.¹⁹ In line with these findings, implants with modified macrogeometry and the presence of healing chambers may minimize the negative influence of surgical trauma, resulting in better wound healing at the bone development stage as confirmed by the occurrence of osteons enclosed by lamellar structures with centric osteocytes, indicating a rapid organization of osseous tissue at implants with a hollow chamber.²⁹ Additionally, researchers support the benefits of healing chambers due to early mineralization and higher bone-implant contact rates observed in implants with modified macrogeometry.²⁹

According to previous findings^{19,29,39,41} and considering the molecular outcomes of this study, it could be hypothesized that in implants with healing chambers, OPN-stimulated mesenchymal stem cell migration may be relevant in earlier phases of peri-implant bone repair and that OPN could also positively affect later bone healing phases, contributing to the mineralization process around these implants.

Other bone biomarkers evaluated in this study were BMP-2, Runx2, β -catenin, Dkk1, and RANKL/OPG. However, no significant impact of implant macrogeometry was demonstrated on the local modulation of these molecules ($p > 0.05$). The absence of differences for these molecules could be related to the period of evaluation of peri-implant bone samples, since this study focused only on an evaluation period after implant placement (30 days). Thus, the molecular findings observed in this trial possibly reflect late events related to peri-implant bone healing. Additional investigations including short-term assessments of osseointegration could be relevant to identifying the impact of modified implant macrogeometry in earlier periods of peri-implant bone repair.

It is well-known that bone formation around implants is influenced by numerous biological and physical mechanisms, which may interfere both on bone-related gene expression and cell differentiation. Although the present research has provided valuable insights into the mechanisms by which implant macrogeometry may interfere on bone healing, additional studies are required to unravel other pathways that can contribute to a better understanding of the role of modified implant macrodesign in bone metabolism. In this context, a limitation of the present study is the absence of osseointegration analysis (microtomography or histomorphometry). This type of assessment allows the evaluation of the bone adjacent to and with a structural/functional connection with the implant. It is important to highlight that, to our knowledge, no other study to date has determined the influence of a healing chamber on molecular changes around

dental implants and further investigations are required to confirm these data.

The implants evaluated in this investigation presented surface modifications with moderately microtextured features; the only variable was implant macrogeometry. Therefore, although the positive outcomes achieved by the test implants in this study are attributed to the modified implant macrogeometry, it is relevant to highlight that the combination of modified implant surface and the presence of a healing chamber could provide “cumulative” positive effects on the osseointegration process.⁴² It has been hypothesized that this combination may achieve a hybrid healing pattern, in which an initial juxtaposition between implant threads and native bone tissue guarantees primary stability, whereas the healing chambers with modified surfaces ensure immediate interaction between clot components (proteins, plasma, and cells) and implant surface, optimizing peri-implant bone formation. This combination seems to be a relevant strategy, where intensive bone remodeling is compensated by fast bone formation within the chamber, probably supporting a biomechanical stability standpoint during all periods of peri-implant bone repair. Additionally, better comprehension of these aspects may provide additional support for the clinical use of this approach to optimize dental implant therapy, mainly at sites with lower bone density or in patients with harmful bone healing.

Conclusion

This study demonstrated that the modified macrogeometry of implants optimizes peri-implant bone repair, favoring the upregulation of OPN expression in the bone tissue around implants.

Acknowledgments

This research was supported by Implacil de Bortoli and by National Council for Scientific and Technological Development (CNPq), Brasília, DF, Brazil [Process 441518/2014-1].

References

1. Moraschini V, Poubel LA, Ferreira VF, Barboza ES. Evaluation of survival and success rates of dental implants reported in longitudinal studies with a follow-up period of at least 10 years: a systematic review. *Int J Oral Maxillofac Implants*. 2015 Mar;44(3):377-88. <https://doi.org/10.1016/j.ijom.2014.10.023>
2. Berglundh T, Abrahamsson I, Lang NP, Lindhe J. De novo alveolar bone formation adjacent to endosseous implants. *Clin Oral Implants Res*. 2003 Jun;14(3):251-62. <https://doi.org/10.1034/j.1600-0501.2003.00972.x>
3. Lioubavina-Hack N, Lang NP, Karring T. Significance of primary stability for osseointegration of dental implants. *Clin Oral Implants Res*. 2006 Jun;17(3):244-50. <https://doi.org/10.1111/j.1600-0501.2005.01201.x>
4. Campos FE, Gomes JB, Marin C, Teixeira HS, Suzuki M, Witek L, et al. Effect of drilling dimension on implant placement torque and early osseointegration stages: an experimental study in dogs. *J Oral Maxillofac Surg*. 2012 Jan;70(1):e43-50. <https://doi.org/10.1016/j.joms.2011.08.006>
5. Freitas AC Jr, Bonfante EA, Giro G, Janal MN, Coelho PG. The effect of implant design on insertion torque and immediate micromotion. *Clin Oral Implants Res*. 2012 Jan;23(1):113-8. <https://doi.org/10.1111/j.1600-0501.2010.02142.x>
6. Jimbo R, Tovar N, Anchieta RB, Machado LS, Marin C, Teixeira HS, et al. The combined effects of undersized drilling and implant macrogeometry on bone healing around dental implants: an experimental study. *Int J Oral Maxillofac Implants*. 2014 Oct;43(10):1269-75. <https://doi.org/10.1016/j.ijom.2014.03.017>
7. Jung RE, Pjetursson BE, Glauser R, Zembic A, Zwahlen M, Lang NP. A systematic review of the 5-year survival and complication rates of implant-supported single crowns. *Clin Oral Implants Res*. 2008 Feb;19(2):119-30. <https://doi.org/10.1111/j.1600-0501.2007.01453.x>
8. Busenlechner D, Fürhauser R, Haas R, Watzek G, Mailath G, Pommer B. Long-term implant success at the Academy for Oral Implantology: 8-year follow-up and risk factor analysis. *J Periodontal Implant Sci*. 2014 Jun;44(3):102-8. <https://doi.org/10.5051/jpis.2014.44.3.102>
9. Chrcanovic BR, Albrektsson T, Wennerberg A. Smoking and dental implants: a systematic review and meta-analysis. *J Dent*. 2015 May;43(5):487-98. <https://doi.org/10.1016/j.jdent.2015.03.003>
10. Dereka X, Calciolari E, Donos N, Mardas N. Osseointegration in osteoporotic-like condition: A systematic review of preclinical studies. *J Periodontal Res*. 2018 Dec;53(6):933-40. <https://doi.org/10.1111/jre.12566>
11. Radi IA, Ibrahim W, Iskandar SM, AbdelNabi N. Prognosis of dental implants in patients with low bone density: a systematic review and meta-analysis. *J Prosthet Dent* 2018; 120:668-677.
12. Komori T. Regulation of proliferation, differentiation and functions of osteoblasts by Runx2. *Int J Mol Sci*. 2019 Apr;20(7):1694. <https://doi.org/10.3390/ijms20071694>
13. Gregory CA, Singh H, Perry AS, Prockop DJ. The Wnt signaling inhibitor dickkopf-1 is required for reentry into the cell cycle of human adult stem cells from bone marrow. *J Biol Chem*. 2003 Jul;278(30):28067-78. <https://doi.org/10.1074/jbc.M300373200>
14. MacDonald BT, Joiner DM, Oyserman SM, Sharma P, Goldstein SA, He X, et al. Bone mass is inversely proportional to Dkk1 levels in mice. *Bone*. 2007 Sep;41(3):331-9. <https://doi.org/10.1016/j.bone.2007.05.009>
15. Simonet WS, Lacey DL, Dunstan CR, Kelley M, Chang MS, Lüthy R, et al. Osteoprotegerin: a novel secreted protein involved in the regulation of bone density. *Cell*. 1997 Apr;89(2):309-19. [https://doi.org/10.1016/S0092-8674\(00\)80209-3](https://doi.org/10.1016/S0092-8674(00)80209-3)
16. Yasuda H, Shima N, Nakagawa N, Yamaguchi K, Kinosaki M, Goto M, et al. A novel molecular mechanism modulating osteoclast differentiation and function. *Bone*. 1999 Jul;25(1):109-13. [https://doi.org/10.1016/S8756-3282\(99\)00121-0](https://doi.org/10.1016/S8756-3282(99)00121-0)
17. Eraslan O, Inan O. The effect of thread design on stress distribution in a solid screw implant: a 3D finite element analysis. *Clin Oral Investig*. 2010 Aug;14(4):411-6. <https://doi.org/10.1007/s00784-009-0305-1>
18. Coelho PG, Jimbo R. Osseointegration of metallic devices: current trends based on implant hardware design. *Arch Biochem Biophys*. 2014 Nov;561:99-108. <https://doi.org/10.1016/j.abb.2014.06.033>
19. Gehrke SA, Dedavid BA, Aramburú JS, Pérez-Díaz L, Calvo Guirado JL, Canales PM, et al. Effect of different morphology of titanium surface on the bone healing in defects filled only with blood clot: a new animal study design. *BioMed Res Int*. 2018 Aug;2018:4265474. <https://doi.org/10.1155/2018/4265474>
20. Casarin RC, Casati MZ, Pimentel SP, Cirano FR, Algayer M, Pires PR, et al. Resveratrol improves bone repair by modulation of bone morphogenetic proteins and osteopontin gene expression in rats. *Int J Oral Maxillofac Implants*. 2014 Jul;43(7):900-6. <https://doi.org/10.1016/j.ijom.2014.01.009>
21. Pimentel SP, Casarin RC, Ribeiro FV, Cirano FR, Rovaris K, Haiter Neto F, et al. Impact of micronutrients supplementation on bone repair around implants: microCT and counter-torque analysis in rats. *J Appl Oral Sci*. 2016;24(1):45-51. <https://doi.org/10.1590/1678-775720150293>
22. Conte A, Ghiraldini B, Casarin RC, Casati MZ, Pimentel SP, Cirano FR, Duarte PM, Ribeiro FV. Impact of type 2 diabetes on the gene expression of bone-related factors at sites receiving dental implants. *Int J Oral Maxillofac Surg*. 2015;44(10):1302-8.

23. Leonard G, Coelho P, Polyzois I, Stassen L, Claffey N. A study of the bone healing kinetics of plateau versus screw root design titanium dental implants. *Clin Oral Implants Res.* 2009 Mar;20(3):232-9. <https://doi.org/10.1111/j.1600-0501.2008.01640.x>
24. Marin C, Granato R, Suzuki M, Gil JN, Janal MN, Coelho PG. Histomorphologic and histomorphometric evaluation of various endosseous implant healing chamber configurations at early implantation times: a study in dogs. *Clin Oral Implants Res.* 2010 Jun;21(6):577-83. <https://doi.org/10.1111/j.1600-0501.2009.01853.x>
25. Coelho PG, Jimbo R, Tovar N, Bonfante EA. Osseointegration: hierarchical designing encompassing the micrometer, micrometer, and nanometer length scales. *Dent Mater.* 2015 Jan;31(1):37-52. <https://doi.org/10.1016/j.dental.2014.10.007>
26. Gehrke SA, Eliers Treichel TL, Pérez-Díaz L, Calvo-Guirado JL, Aramburú Júnior J, Mazón P, et al. Impact of different titanium implant thread designs on bone healing: a biomechanical and histometric study with an animal model. *J Clin Med.* 2019 May;8(6):E777. <https://doi.org/10.3390/jcm8060777>
27. Barros RR, Novaes AB Jr, Papalexiou V, Souza SL, Taba Junior M, Palioto DB, et al. Effect of biofunctionalized implant surface on osseointegration: a histomorphometric study in dogs. *Braz Dent J.* 2009;20(2):91-8. <https://doi.org/10.1590/S0103-64402009000200001>
28. Bonfante EA, Granato R, Marin C, Suzuki M, Oliveira SR, Giro G, et al. Early bone healing and biomechanical fixation of dual acid-etched and as-machined implants with healing chambers: an experimental study in dogs. *Int J Oral Maxillofac Implants.* 2011;26(1):75-82.
29. Meirelles L, Brånemark PI, Albrektsson T, Feng C, Johansson C. Histological evaluation of bone formation adjacent to dental implants with a novel apical chamber design: preliminary data in the rabbit model. *Clin Implant Dent Relat Res.* 2015 Jun;17(3):453-60. <https://doi.org/10.1111/cid.12139>
30. Yamazaki M, Nakajima F, Ogasawara A, Moriya H, Majeska RJ, Einhorn TA. Spatial and temporal distribution of CD44 and osteopontin in fracture callus. *J Bone Joint Surg Br.* 1999 May;81(3):508-15. <https://doi.org/10.1302/0301-620X.81B3.0810508>
31. Giachelli CM, Steitz S. Osteopontin: a versatile regulator of inflammation and biomineralization. *Matrix Biol.* 2000 Dec;19(7):615-22. [https://doi.org/10.1016/S0945-053X\(00\)00108-6](https://doi.org/10.1016/S0945-053X(00)00108-6)
32. Scatena M, Liaw L, Giachelli CM. Osteopontin: a multifunctional molecule regulating chronic inflammation and vascular disease. *Arterioscler Thromb Vasc Biol.* 2007 Nov;27(11):2302-9. <https://doi.org/10.1161/ATVBAHA.107.144824>
33. Duvall CL, Taylor WR, Weiss D, Wojtowicz AM, Guldberg RE. Impaired angiogenesis, early callus formation, and late stage remodeling in fracture healing of osteopontin-deficient mice. *J Bone Miner Res.* 2007 Feb;22(2):286-97. <https://doi.org/10.1359/jbmr.061103>
34. Zou C, Song G, Luo Q, Yuan L, Yang L. Mesenchymal stem cells require integrin $\beta 1$ for directed migration induced by osteopontin in vitro. *In Vitro Cell Dev Biol Anim.* 2011 Mar;47(3):241-50. <https://doi.org/10.1007/s11626-010-9377-0>
35. Hunter GK. Role of osteopontin in modulation of hydroxyapatite formation. *Calcif Tissue Int.* 2013 Oct;93(4):348-54. <https://doi.org/10.1007/s00223-013-9698-6>
36. Chen Q, Shou P, Zhang L, Xu C, Zheng C, Han Y, et al. An osteopontin-integrin interaction plays a critical role in directing adipogenesis and osteogenesis by mesenchymal stem cells. *Stem Cells.* 2014 Feb;32(2):327-37. <https://doi.org/10.1002/stem.1567>
37. Ayukawa Y, Takeshita F, Inoue T, Yoshinari M, Shimono M, Suetsugu T, et al. An immunoelectron microscopic localization of noncollagenous bone proteins (osteocalcin and osteopontin) at the bone-titanium interface of rat tibiae. *J Biomed Mater Res.* 1998 Jul;41(1):111-9. [https://doi.org/10.1002/\(SICI\)1097-4636\(199807\)41:1<111::AID-JBM14>3.0.CO;2-Q](https://doi.org/10.1002/(SICI)1097-4636(199807)41:1<111::AID-JBM14>3.0.CO;2-Q)
38. Puleo DA, Nanci A. Understanding and controlling the bone-implant interface. *Biomaterials.* 1999 Dec;20(23-24):2311-21. [https://doi.org/10.1016/S0142-9612\(99\)00160-X](https://doi.org/10.1016/S0142-9612(99)00160-X)
39. Raheja LF, Genetos DC, Yellowley CE. Hypoxic osteocytes recruit human MSCs through an OPN/CD44-mediated pathway. *Biochem Biophys Res Commun.* 2008 Feb;366(4):1061-6. <https://doi.org/10.1016/j.bbrc.2007.12.076>
40. Zou C, Luo Q, Qin J, Shi Y, Yang L, Ju B, et al. Osteopontin promotes mesenchymal stem cell migration and lessens cell stiffness via integrin $\beta 1$, FAK, and ERK pathways. *Cell Biochem Biophys.* 2013 Apr;65(3):455-62. <https://doi.org/10.1007/s12013-012-9449-8>
41. Natoli RM, Yu H, Meislin MC, Abbasnia P, Roper P, Vuchkovska A, et al. Alcohol exposure decreases osteopontin expression during fracture healing and osteopontin-mediated mesenchymal stem cell migration in vitro. *J Orthop Surg Res.* 2018 Apr;13(1):101. <https://doi.org/10.1186/s13018-018-0800-7>
42. Nevins M, Chu SJ, Jang W, Kim DM. Evaluation of an Innovative Hybrid Macrogeometry Dental Implant in Immediate Extraction Sockets: A Histomorphometric Pilot Study in Foxhound Dogs. *Int J Periodont Restor Dent.* 2019;39(1):29-37. <https://doi.org/10.11607/prd.3848>